CrossMark

Thermodynamic aspects of freeze-drying

A case study of an "organic solvent–water" system

A. G. Ogienko[1,2] · V. A. Drebushchak[2,3] · E. G. Bogdanova[1,2] · A. S. Yunoshev[2,4] ·
A. A. Ogienko[5] · E. V. Boldyreva[6] · A. Yu. Manakov[1,2]

Abstract Aqueous solutions of glycine and tetrahydrofuran (THF) were frozen under variable conditions and subsequently annealed. The phases that resulted from this process were studied by X-ray diffraction, DSC and cryotemperature SEM. Under conditions achieved in common laboratory freeze-dryers, the THF clathrate hydrate of cubic structure II was formed in near-quantitative yields. The temperature–composition state diagram for the THF–water–β-glycine systems suggests that the critical temperature of the primary drying stage is the temperature of the four-phase peritectic reaction (269 K), and not the temperature of the congruent melting of the THF hydrate in the THF–water system (278 K). Freeze-drying is shown to go much faster if aqueous solutions are substituted for THF–water solutions. This finding is of great importance for practical applications, including pharmaceutical drug formulation.

✉ A. G. Ogienko
andreyogienko@gmail.com

✉ E. V. Boldyreva
eboldyreva@yahoo.com

1   Nikolaev Institute of Inorganic Chemistry SB RAS, Lavrentiev Ave. 3, Novosibirsk, Russia 630090

2   Novosibirsk State University, ul. Pirogova 2, Novosibirsk, Russia 630090

3   Sobolev Institute of Geology and Mineralogy SB RAS, Novosibirsk, Russia 630090

4   Lavrentiev Institute of Hydrodynamics SB RAS, Novosibirsk, Russia 630090

5   Institute of Cytology and Genetics SB RAS, Novosibirsk, Russia 630090

6   Institute of Solid State Chemistry and Mechanochemistry SB RAS, ul. Kutateladze 18, Novosibirsk, Russia 630128

Introduction

Freeze-drying (lyophilization) is a drying technology widely used in the pharmaceutical industry [1]. It provides products with desired physicochemical properties, such as enhanced dissolution rates and bioavailability, and allows for the preservation and stabilization of thermolabile active pharmaceutical ingredients (APIs) and biologicals that have limited shelf life in solution [2–4]. It is important that product temperature during lyophilization remains below the characteristic glass transition/eutectic melting temperatures of amorphous/crystalline phases. Otherwise, above the glass transition temperature the amorphous phase turns oily and cannot support its own mass (collapse temperature), whereas above the eutectic melting temperature a liquid phase is formed, resulting in a massive loss of porous structure of the powdered material. Visually, the loss of structure of the dried matrix causes "cake collapse" in the freeze-dried product [4] and API recrystallizes into larger crystals of the same or other phases with drastic decrease of surface area.

Water is the most commonly used solvent in the freeze-drying method. However, scarce solubility of some hydrophobic and insoluble APIs in water severely limits the application of freeze-drying using aqueous solutions. This has led to the recent investigation of pure organic solvents or mixed organic–water solvents (further in the text termed «organic–water co-solvent systems») for use in freeze-drying processes. The use of a single-component organic solvent makes it impossible to prepare a stock solution containing water-soluble components, such as

buffer salts or low-molecular mass carriers (mannitol, lactose, leucine, glycine, etc.). These are important solutions as they are used for producing solid dispersions to improve solubility for oral and/or intravenous drug delivery, and to enhance aerosolization properties of dry powder inhaler formulations [5]. In contrast, employment of organic–water co-solvent systems in the freeze-drying process facilitates manufacture of the stock solution by increasing the wettability and solubility of APIs, increasing sublimation rates, decreasing reconstitution times, and improving freeze-dried product stability [5–8].

To use organic–water co-solvent systems, it is necessary to find optimal compositions and concentrations of stock solutions, as well as optimal conditions for all stages of the freeze-drying cycle (freezing, annealing, primary drying, secondary drying). Moreover, most organic–water co-solvent solutions do not freeze in typical laboratory refrigerators because of their very low eutectic temperatures. Potential alternative methods for solidifying organic–water solutions are variants of cryogenic technologies, such as spray freeze-drying (SFD), spray-freezing into liquid (SFL) or thin film freezing (TFF) [9–11]. In these methods, the solution containing with API is sprayed either directly into a cryogenic liquid, usually liquid nitrogen (SFD, SFL), or over a cryogenically cooled solid surface (TFF). In the case of using some hydrophilic solvents (such as DMSO, ethanol, acetone, etc.) for mixed organic–aqueous solutions [12–14], the frozen species obtained by cryogenic technologies still have eutectic temperatures considerably lower than those available in typical pilot or laboratory freeze-dryers. Therefore, on attempted freeze-drying liquid phases containing significant amounts of associated water (solutions of water in the organic solvent) are formed. As a result, these formulations are nearly impossible to dry and unacceptable freeze-dried cakes are formed. The undesirable consequences include poor appearance, collapse, reconstitution of the samples, as well as a drastic degradation of the drug therapeutic activity.

To avoid formation of liquid phases, one needs to study the thermodynamics and kinetics of the processes related to all stages of freeze-drying. A phase diagram of the selected organic–water co-solvent system gives optimized parameters of a freeze-drying cycle only in the first approximation. Depending on the number of components (API, excipient), it is important to consider the relevant ternary/quaternary system in combination with corresponding binary systems (API-solvent, API-water, etc.). Further, one must also study the possibility of API/excipient hydrate (solvate) formation [15, 16]. In organic–water co-solvent systems, hydrates (water–TBA/ethanol/DMSO) [12, 13, 17] or clathrate hydrates (water–acetone/THF/1,4-dioxane) [14] can be formed on cooling. Clathrate hydrates are water-based crystalline compounds consisting of a lattice-like

framework of hydrogen-bonded water molecules that form cavities, in which small (usually <0.9 nm) non-polar guest molecules of gases or volatile organics are incorporated [18]. Whereas clathrate hydrates of natural gases are widely applied for energy storage and transportation [19], there are limited reports on intentional use of clathrate hydrates for pharmaceutical applications [20–23].

Of common organic–water co-solvent systems, TBA–water is of particular interest and has been successfully employed in the commercial manufacture of CAVERJECT® Sterile Powder [24]. This co-solvent system is characterized by its low toxicity, its high eutectic melting point, thermal stability of hydrates that form on freezing, its low sublimation enthalpy and high vapor pressure. Further, the morphology of ice crystals formed on freezing accounts for a relatively low resistance of the partially dried solids to penetration of water vapor on sublimation. All these factors increase the sublimation rate of the TBA–water system [5–8, 24–26].

To develop new lyophilized API/protein formulations, one needs to study the phase diagram of the TBA–water–API ternary system. However, obtaining such a diagram—even in a limited concentration range—is complicated. The phase composition of the frozen TBA–water solutions does not correspond to that calculated from the binary TBA–water phase diagram (the formation of hydrates is not complete, a metastable hydrate is formed) and depends on the cooling rate [6, 17, 27]. Of further complication is the fact that crystallization of TBA and TBA hydrate is inhibited by the presence of excipients, such as sucrose and mannitol [24]. Even if, for simplicity, we neglect the presence of an API, a series of the intermediate phases can be formed in the TBA–water-excipient system, depending on the choice of excipient, the composition of the starting solution and the cooling conditions. As two extreme cases, one can propose two results, (a) ice Ih is the only crystalline phase, while the excipient, TBA and unfrozen water are amorphous, or (b) ice Ih, hydrates TBA·2H$_2$O and TBA·7H$_2$O (metastable) and a hydrate/solvate of the excipient are all crystalline, whereas both the excipient and TBA are amorphous; liquid water remains in this case. Potential consequences of these complex and poorly reproducible phase compositions are vial-to-vial variation in drying rates, collapse temperatures and residual TBA and water content in the final lyophiles [15, 24, 28, 29]. A large number of possible parameters must be varied empirically before optimum conditions can be found.

We supposed another organic solvent—water system, namely, the THF–water, to be not only easier to study, but also potentially more promising for practical applications. This is one of the best studied systems in relation to the chemistry of clathrate hydrates. The THF clathrate hydrate (cubic structure II (CS-II), Fd3m, $a \sim 17.1$ Å, molar ratio

THF/water equal to 1:17) [14] crystallizes on cooling from a homogenous aqueous solution. The THF clathrate hydrate is stable up to fairly high temperatures (278 K, while the eutectic temperature in this system is 164 K) [14], thus making it possible to carry out freeze-drying across a certain concentration range at significantly higher temperatures.

Compared to the TBA–water–sucrose/lactose system [5–7, 17], when substituting TBA for THF, we have additionally substituted sucrose or lactose for glycine, a commonly used bulking agent in freeze-dried formulations. In contrast to sucrose or lactose, which tends to remain amorphous during lyophilization [30], glycine forms crystalline phases either directly on freezing, or as a result of subsequent annealing [30–33]. The main advantage of substituting the TBA–water–sucrose system for THF–water–glycine system is the possibility to prepare solutions with concentrations that give only 3, and in some cases only 2, crystalline (and no amorphous) phases on freezing or on freezing and subsequent annealing. It should also be noted that the physical state of the final lyophiles is the most important determinant of residual moister/organic solvent level [28, 30].

The aim of the present work was to study the phase diagram of the THF–water–glycine system along with the formation of the THF clathrate hydrate. The ternary phase diagram determination is essential in designing freeze-dried formulations and processes parameters for systems with a crystalline solute such as glycine [34]. In doing so, this study demonstrates parameter optimization for a freeze-drying cycle.

Experimental

Materials

Glycine (JSC "Reakhim") was recrystallized to obtain pure α-form as described in [35]. Peroxide-free twice-distilled THF (JSC "VEKTON") and distilled water were used as solvents.

Samples for low-temperature powder X-ray diffraction and DSC

Starting solutions glycine (5 mass%) in the THF/water co-solvent system (THF hydrate composition, 20 mass% of THF), THF–water solutions (20 mass%) (reference solution), aqueous glycine solutions (5 mass%) (reference solution). Freezing methods:

Method 1 Vials (Sci/Spec, B69308), 1 mL aliquots, air thermostat, 250 K (freezing time ca. 1 h).

Method 2 Vials (Sci/Spec, B69308), 1 mL aliquots, cryothermostat (KRYO-VT-05-02, TERMEX, Russia), 220 K (freezing time ca. 1 min).

Immediately after freezing the solutions (methods 1, 2) a few vials were broken under liquid nitrogen temperatures, in order to extract the samples, which were thereafter kept in liquid nitrogen until diffraction experiments (hereafter "frozen": 1a, 2a). The other vials of these series were placed into an air thermostat at 250 K overnight for annealing (hereafter "annealed": 1b, 2b).

Method 3 Small amounts of solution were splashed onto a copper plate cooled to liquid nitrogen temperature (freezing time ca. 1 s). The frozen solution was gently ground manually at liquid nitrogen temperature and was divided into two parts—one was kept in liquid nitrogen before diffraction experiments (hereafter "frozen": 3a), a second was placed into an air thermostat at 250 K overnight (hereafter "annealed": 3b).

Samples for drying rate determination and cryotemperature scanning electron microscopy (cryo-SEM)

Glycine solutions (5 mass%) in the THF/water co-solvent system were prepared by mass (5, 10, 15, 20 mass% of THF). An aqueous glycine solution served as the control. In each series, the solutions were put into ten vials (19 × 65 mm, 11 mL; Sci/Spec, B69308); the mass of the solution in each vial was 1.00 ± 0.05 g (vial fill depth of 5 mm, inner diameter standard and equal to 16.5 mm). Then the vials were tightly closed with a PTFE cap and placed into an air thermostat at 250 K overnight (12 h) before any further experiments.

Methods

Powder X-ray diffraction (PXRD)

PXRD experiments were aimed to: (a) identify the phases formed on cooling of glycine solutions in water and THF/water co-solvent system; (b) characterize final solid products. We used a Bruker D8 Advance diffractometer ($\lambda = 1.5406$ Å, tube voltage of 40 kV and tube current of 40 mA) equipped with an Anton Paar TTK 450 low-temperature chamber permitting work under vacuum down to 10^{-3} Torr. The vial with frozen solution was broken, the sample was gently ground in a mortar (all operations being performed at liquid nitrogen temperature) and placed onto a holder, which had been preliminary cooled to 130 K. Diffraction patterns were measured in the 150–280 K temperature range (2Θ scans from 5° to 45°, 0.02° step, approximately 8 min per pattern).

DSC

Samples of a frozen glycine solution were ground in a metal mortar cooled with liquid nitrogen, then loaded into a standard aluminum crucible (DSC-204 Netzsch, 25 μL) and also pre-cooled with liquid nitrogen. Sample mass varied from 0.16 to 2 mg. It is usual to measure the sample mass by weighing the crucible before and after loading the sample in it. Here, however, this was impossible because the sample must always be kept below 273 K. Therefore, we weighed the empty crucible, filled it with a sample, carried out the experiments, and only then weighed it again. The crucible filled with the sample was inserted into the DSC cell at 190 K. The heat flow sensor of the DSC showed an endothermic effect at that moment, proving that the crucible was below 190 K. The measurements were taken at different heating rates, 1 K min^{-1} (near 270 K), $2 \div 3$ K min^{-1} (near 170 K) and 6 K min^{-1} (crystallization near 220 K), with a flow of pure Ar of 15 mL min^{-1}.

Measurement of drying rate

Measurements of the drying rate were accomplished with a laboratory-scale freeze-dryer (one processing shelf, 25.0×35.0 cm, with temperature range of 240–350 K) (NIIC SB RAS, Russia) equipped with an organic solvent trap. A Convection-enhanced Pirani gauge [275 Mini-Convectron® (Granville-Phillips®)] was used to monitor the chamber pressure. The shelf was equilibrated at 268 K before vials were loaded and then placed under vacuum. Freeze-drying was carried out until the pressure dropped to $P < 14$ mTorr [DUO 60A (Pfeiffer Balzers)]. After that, the shelf temperature was increased to 303 K and held for 2 h. The pressure in the freeze-dryer was subsequently increased to $P = 1$ bar by filling it with dry nitrogen. Upon removal from the freeze-dryer, samples were stored in a vacuum desiccator over phosphorus pentoxide.

Blank test

Ten weighed vials with frozen (method 1) aqueous glycine (5 mass%) solution (1.00 ± 0.05 g per vial) were placed onto a preliminarily cooled shelf (268 K). Freeze-drying was carried out until the pressure dropped to $P < 14$ mTorr. The pressure in the freeze-dryer was then increased to $P = 1$ bar by filling it with dry nitrogen. The vials were removed from the freeze-dryer, closed, warmed to room temperature and weighed. Glycine: $m_{calc.} = 0.4843$ g; $m_{exp.} = 0.4663$ g.

Scanning electron microscopy (SEM)

The direct observation method by SEM was used to characterize the morphology of the frozen solutions. To extract a sample, the vial was carefully broken in the vessel with the liquid nitrogen temperature and the sample was placed on a brass holder, which had been already cooled to liquid nitrogen temperatures. Horizontal sample cuts were prepared that corresponded to a cross section of the cylindrical sample frozen in the vials. The holder was then placed into a staffing hole of an SEM TM-1000 (Hitachi) sample holder. It was determined experimentally that the sample temperature did not rise above 110 K during running.

Morphological examination of the lyophilized glycine samples was carried out with an EVO MA10 (Carl Zeiss) scanning electron microscope. The samples were mounted on a SEM stub with double-sided carbon tape and coated with gold to a thickness of about 8 nm with a JFC-1600 Auto Fine Coater (Jeol).

Results and discussion

Powder X-ray diffraction and DSC of the frozen solutions

The results of the low-temperature X-ray diffraction and DSC studies of the THF–water, glycine–water and glycine–THF–water solutions frozen under varying degrees of supercooling can be summarized as follows:

1. Cooling glycine solutions in THF/water co-solvent system (20 mass% THF) in vials (methods 1a, 2a) results in the crystallization of β-glycine (Fig. 1). Similar results have been observed for aqueous glycine solutions frozen at different cooling rates [31, 32]: DSC data indicated only the eutectic β-glycine–ice Ih. When the solution was quench-cooled by splashing it onto a copper plate that was cooled to liquid nitrogen temperatures (method 3a) (the highest cooling rate), glycine formed an amorphous freeze concentrate [31, 33] (Fig. 1).

Warming does not alter the powder diffraction patterns of samples frozen in vials (methods 1a, 2a), but some reflections of the low-temperature X-phase of glycine [31, 33] can be seen in the pattern of the sample prepared by method 3a and recorded at 210 K. On further warming (annealing), the reflections of β-glycine emerge in the PXRD patterns (Fig. 2). At the same time, the DSC curve of the sample prepared by method 3a shows a combination of thermal effects within the temperature range of 210–230 K (Fig. 3); similar results have been observed for the quench-frozen aqueous glycine solution [33]. Therefore, in solutions of the THF/water co-solvent system (method 3a), glycine undergoes a sequence of transformations: glassy/amorphous glycine → "X-phase" → β-glycine, as it does in the case of aqueous solutions [33].
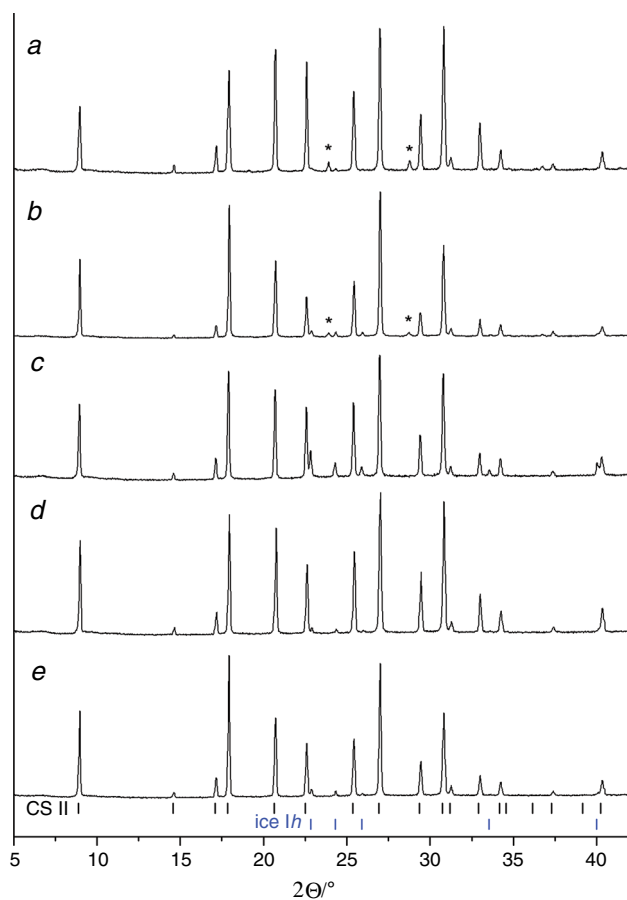
Fig. 1 PXRD patterns (recorded at 150 K): "*a*", "*b*" and "*c*"—powder diffraction patterns of frozen (a—method 1a; b—method 2a, c—method 3a) glycine solutions in THF/water co-solvent system (20 mass% of THF); "*c*" and "*d*"—powder diffraction patterns of frozen (*c*—method 1a; *d*—method 2a) THF–water solutions (20 mass% of THF), used as reference. Low intensity peaks (2*Θ* range ∼22.5°–26°) on patterns "*b*"–"*e*" correspond to ice I*h*. The positions of the reflections of the THF hydrate (CS-II) and ice I*h* are shown as ticks at the *bottom. Asterisks*—the strongest reflections of the *β*-glycine on the patterns "*a*" and "*b*"

2. The common feature of the DSC curves in all samples (methods 1–3) is a thermal effect at 269.1 K (melting of the eutectic ice I*h*–*β*-glycine occurs at 269.9 K) [36] (Fig. 4).

A good agreement between the temperature dependences of unit cell parameters of ice I*h* and THF hydrate obtained in our experiments with the literature data [37–39] (Fig. 5) proves the applicability of the experimental procedure used in this work.

Phase diagram modeling

The results of the DSC experiments cannot be explained, assuming that the polythermal section "THF hydrate–*β*-glycine" of the state diagram of the THF–water–*β*-glycine
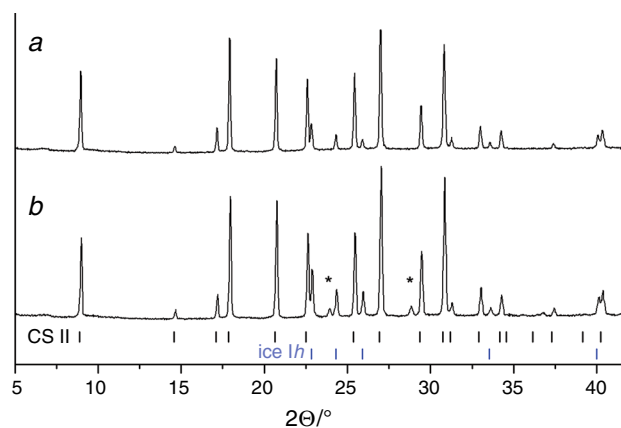

Fig. 2 PXRD patterns (recorded at 150 K) of the frozen (*a*—method 3a, *b*—method 3b) glycine solution in THF/water co-solvent system (20 mass% of THF). The positions of the reflections of the THF hydrate (CS-II) and ice I*h* are shown as ticks at the *bottom. Asterisk*s—the strongest reflections of the *β*-glycine

ternary system is quasi-binary (i.e., assuming that *β*-glycine is an indifferent phase relative to the THF hydrate) (Fig. 6a). In the case of solution with composition of stoichiometry of the THF hydrate, the temperature of the congruent melting of the THF hydrate (278 K) is allowed as the maximum sample temperature during primary drying (Figs. 6a1, 7a1). If the composition of the solution corresponds to the THF hydrate–water subsystem (THF < ∼20 mass%), the maximum allowable sample temperature during primary drying is the temperature of the eutectic melting of the THF hydrate–water system (271.7 K). The additional limitation is the eutectic temperature of the solute (*β*-glycine)–water subsystem (Figs. 6a2, 3, 7a2, 3).

Therefore, we considered possible models of the state diagram of this system. Based on the experimental data and the suggested model (Fig. 6b), we conclude that the addition of the third component (*β*-glycine) changes the melting behavior of the THF hydrate. Melting of the THF hydrate in the THF–water binary system is congruent, whereas melting of the THF hydrate in the water–THF–glycine ternary system is incongruent. The thermal effect at 269.1 K corresponds to the four-phase peritectic reaction (T_P): THF hydrate$_{(solid)}$ + *β*-glycine$_{(solid)}$ = ice I*h*$_{(solid)}$ + solution. Thermal effects at 275–277 K (T_H) are common to all samples and correspond to the melting of the THF hydrate (THF hydrate$_{(solid)}$ = solution) in the ternary system (in the THF–water system, the melting point of the THF hydrate is 278 K) [14]. Thermal effect at ∼164 K observed in the DSC curves of the samples prepared by methods 1, 2 (Figs. 3, 4; Table 1) corresponds to the melting of the ternary eutectic (T_E) in the THF–water–*β*-glycine ternary system (melting temperature of pure THF is 164.76 K) [40].
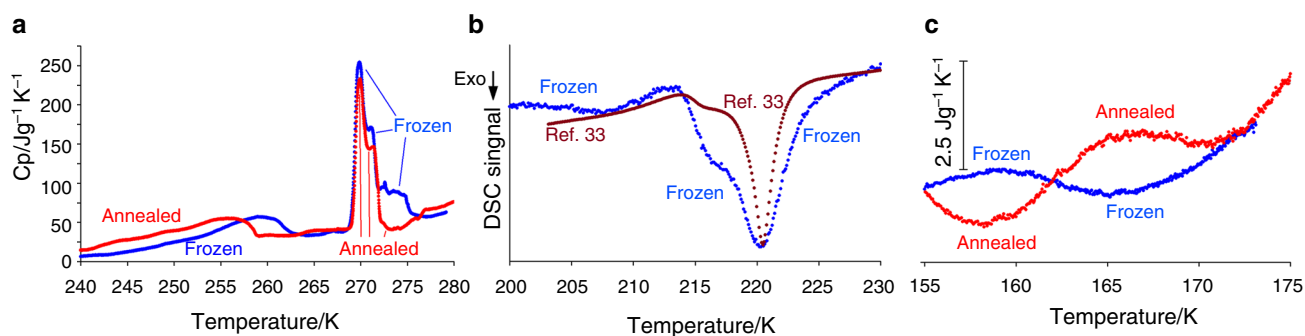
Fig. 3 DSC curves of the frozen glycine solutions (method 3; frozen—method 3a; annealed—method 3b) in THF/water co-solvent system
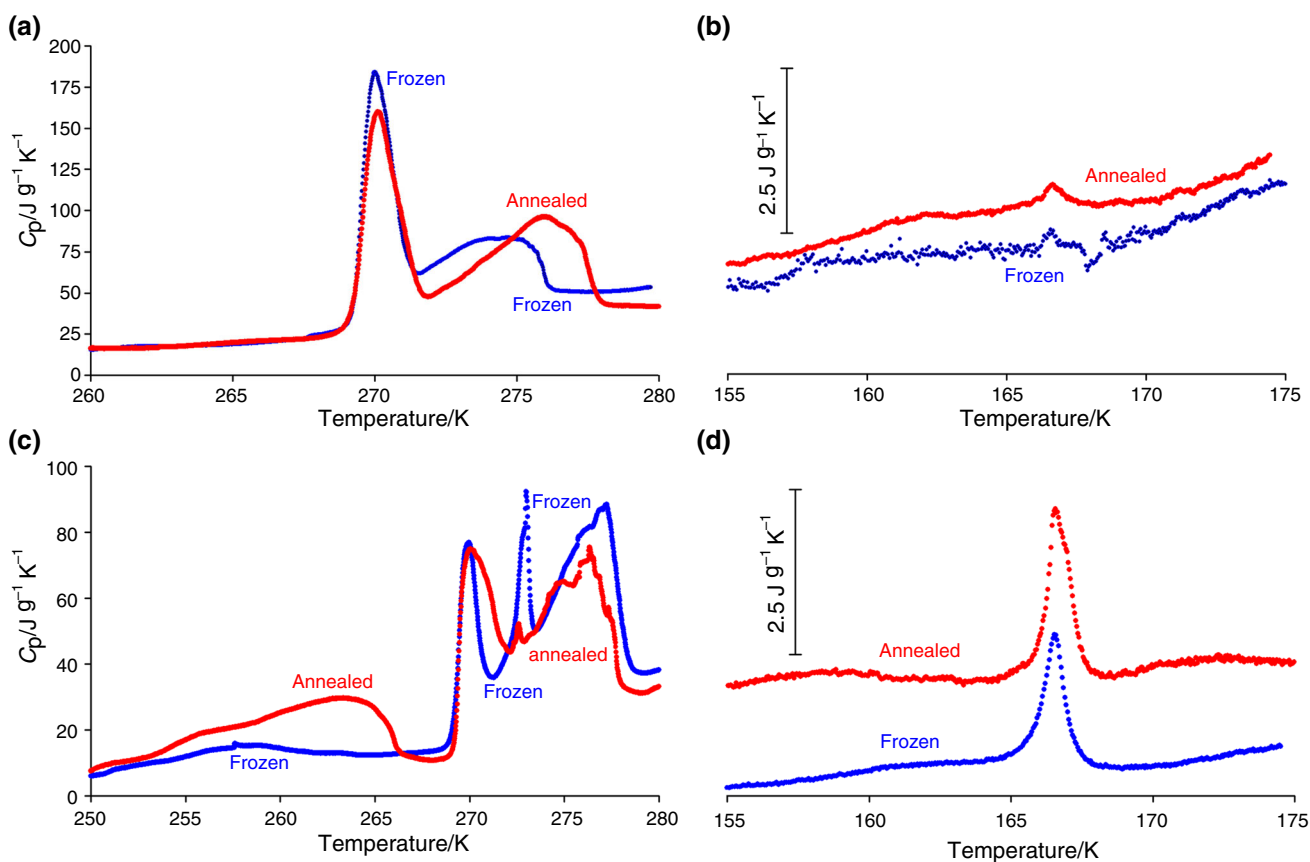

Fig. 4 DSC curves of the frozen glycine solutions in THF/water co-solvent system (20 mass% of THF) (**a, b**—method 1; **c, d**—method 2; frozen—methods 1a, 2a; annealed—methods 1b, 2b)

The effects observed at ~ 272 K (T_1) for samples prepared by methods 2, 3 correspond to the secondary melting [41] of the THF hydrate–ice Ih in the ternary system: THF hydrate$_{(solid)}$ + ice I$h_{(solid)}$ = solution. The thermal effects registered within 255–265 K (T_L) for the samples prepared by methods 2, 3 correspond to the transition of the imaging point (state point is defined as a position on the phase diagram representing a specific set of state variables) of the system from the ternary field THF hydrate–ice Ih–β-glycine to the binary field THF hydrate-liquor (shown by a dashed line in Fig. 7b1). The variation of the ratios of the

thermal effects within 269–276 K for samples prepared by methods 2a/2b and 3a/3b indicates that on fast cooling the imaging point of the system diverts from the THF hydrate–β-glycine line. Besides, the presence of ice Ih reflections in the diffraction patterns of samples prepared by methods 3a/3b suggests partial evaporation of THF on freezing of the solution on the copper plate cooled to liquid nitrogen temperature. Therefore, each of the samples prepared by methods 2a and 3a can be considered as a combination of three states (the line THF hydrate–β-glycine; the subsystem THF hydrate–ice Ih–β-glycine; the subsystem THF
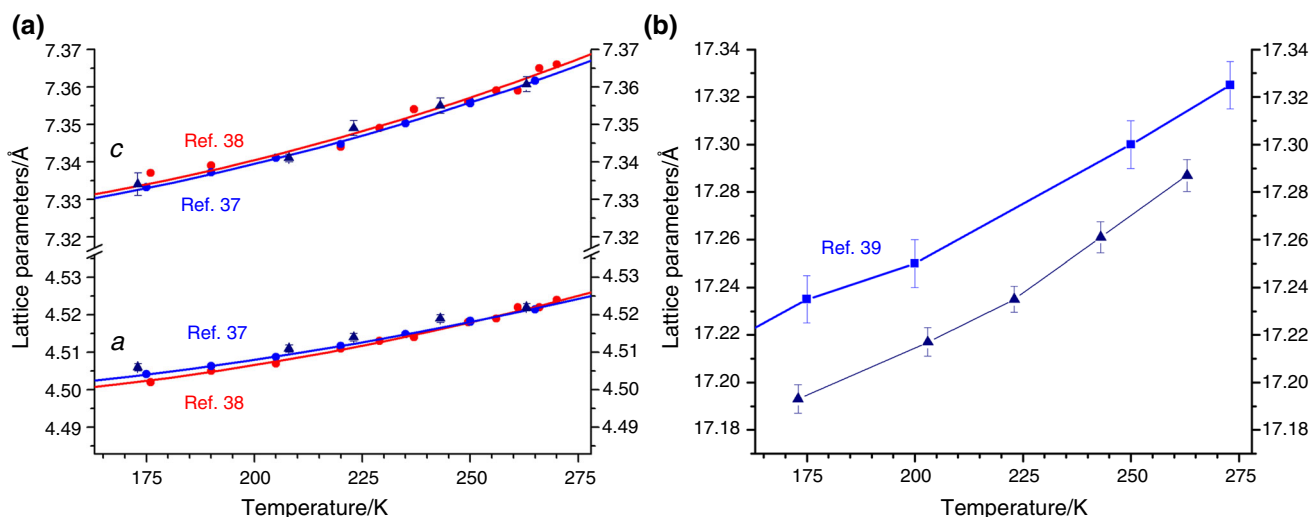
Fig. 5 Comparison of unit cell parameters of ice I*h* (**a**) and THF hydrate (**b**) between 173 and 268 K obtained and in this work (*triangles*) and by Röttger et al. [37] (ice I*h*), Ogienko et al. [38] (ice I*h*) and Hester et al. [39] (THF hydrate)
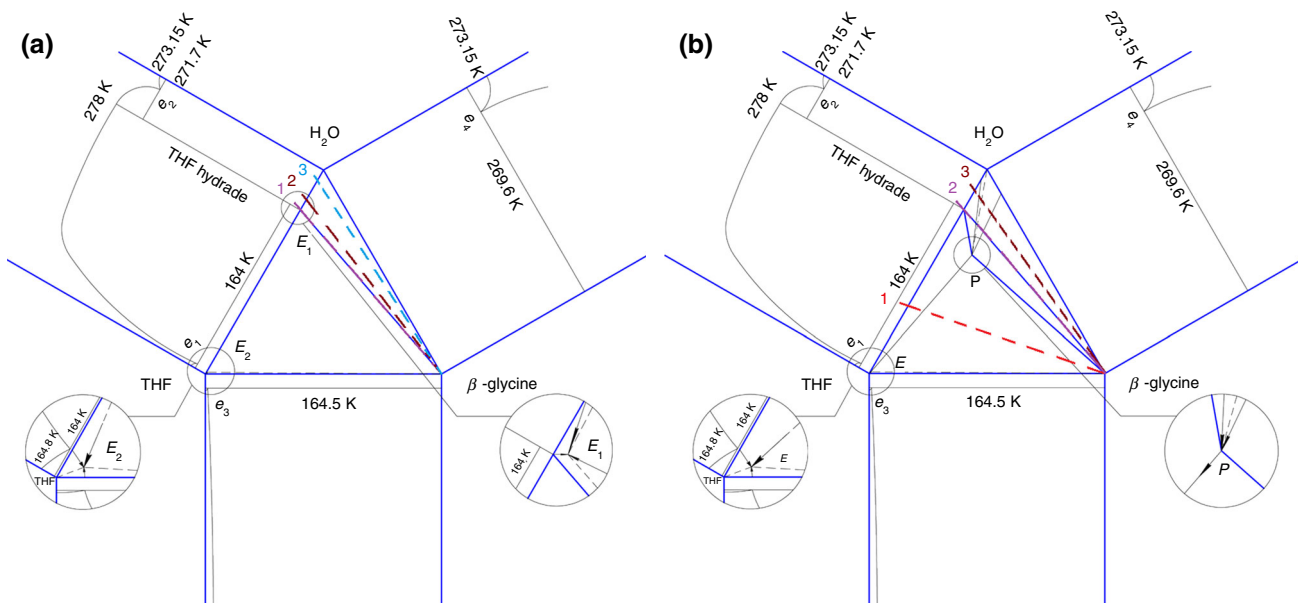

Fig. 6 I. Projections of the "ideal variant" (**a**) and the suggested model (**b**) of the temperature-composition state diagram for the "THF–water–β-glycine" ternary system (modeled in view of literature data [14, 36, 40]) on the composition *triangle*. Arrows in callouts designate the lowering of the temperatures of binary eutectics near the ternary peritectic and the ternary eutectic. Possible polymorphic transformations of glycine in the two- and three-phase fields containing liquid phases are neglected for clarity. *Designations* H—hydrate; I*h*—ice I*h*; Gly—β-glycine; *l*—solution; e_1, e_2, e_3, e_4—binary eutectics; E, E_1, E_2, P—ternary eutectics and ternary peritectic, respectively

hydrate–THF-β-glycine), so that the system is not in equilibrium (Fig. 7b1–b3).

The presence of only two thermal effects in the DSC curves (T_P, T_H) within the temperature range of 269–276 K, very weak (comparable to noise) reflections of ice I*h* in the PXRD patterns of the samples prepared by method 1, as well as the ratio of thermal effects observed at 166 K and within 269–276 K indicate virtually complete

(99.95%) formation of the THF hydrate under these conditions (Figs. 1, 3, 4; Table 1).

Three important conclusions can be made. (1) The THF hydrate forms almost quantitatively under conditions provided by typical laboratory freeze-dryers (method 1); (2) substitution of a single-component solvent (water) by a two-component one (THF–water) does not affect the polymorphism of glycine; (3) the limiting stage of freeze-
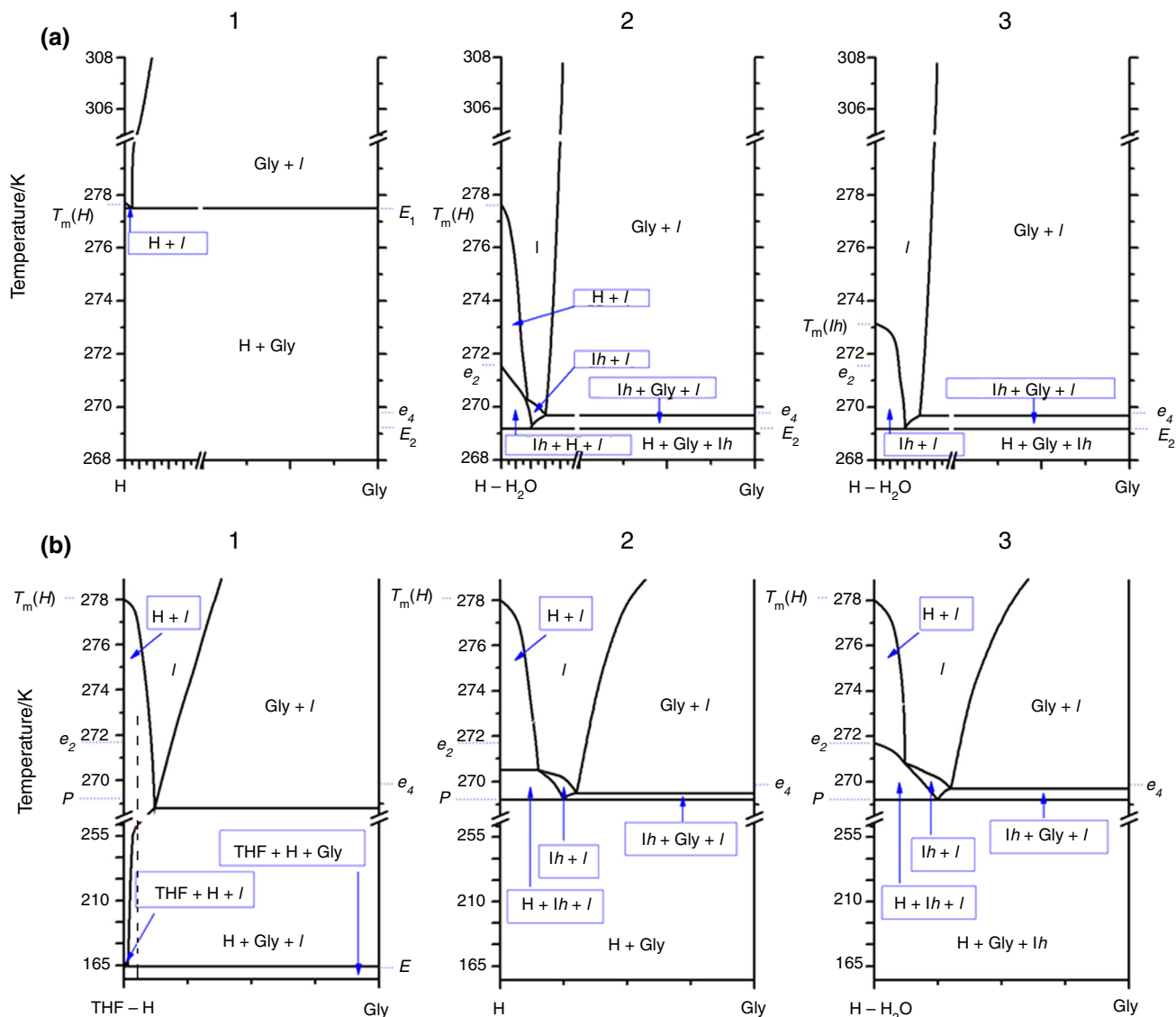
Fig. 7 Polythermal sections of the "ideal variant" (**a**) and the suggested model (**b**) of the state diagram of the "THF–water–β-glycine" ternary system (**a** 1—"H–β-glycine" (line "1" on Fig. 6a); 2, 3—"H–water subsystem–β-glycine" (lines "2" and "3" on Fig. 6a); **b** 1—'"THF–H subsystem"—β-glycine' (line "1" on Fig. 6b); 2—"H–β-glycine" (line "2" on Fig. 6b); 3—'"H–water subsystem"–β-glycine' (line "3" on Fig. 6b)). *Designations* H—hydrate; Ih—ice Ih; Gly—β-glycine; l—solution; e_1, e_2, e_3, e_4—binary eutectics; E, E_1, E_2, P—ternary eutectics and ternary peritectic, respectively; $T_m(H)$, $T_m(Ih)$—THF hydrate and ice Ih melting temperatures, respectively

drying is now the removal of the THF hydrate by sublimation at temperatures below the temperature of the four-phase peritectic reaction (269 K), but not the temperature of the congruent melting of the THF hydrate in the THF–water system (278 K).

Characteristics of frozen solutions

Freezing is a very critical step in the freeze-drying process that strongly influences the following primary and secondary drying stages and, ultimately, the quality of the final lyophilized product [42–44].

Cryo-SEM indicated obvious morphological differences of the frozen samples of glycine solutions, depending on THF content. Some typical images representing the most characteristic trends for each sample are selected and shown in Fig. 8. The examined surfaces were horizontal cuts made across the frozen cylinder formed in the vial. The presence of large (>100 μm) directional (dendrite type) ice crystals and the freeze-concentrated solute phase (frozen β-glycine–ice Ih eutectic) filling the space between the ice crystals was confirmed in the sample of aqueous glycine solution (Fig. 8a). These observations were in good agreement with previous results reported for nucleation of

Table 1 DSC results for frozen glycine solutions in THF/water co-solvent system (20 mass% of THF)

Freezing method	T_E/K	ΔH/J g^{-1}	T_L/K	T_P/K	T_1/K	T_H/K	ΔH/J g^{-1}
Method 1							
a	164.5	0.12	247.5	269.2		275	267
b	164.5		257.2	269.2		276.1	
Method 2							
a	164.1	2.03	259	269.2	272.1	277.2	322
b	164.4		263.2	269.2	272.3	276.3	
Method 3							
a	–	–	256	269.1	271.2		
b	–	–	259	269.2	271.4		

T_E, T_P—ternary eutectic and ternary peritectic melting temperatures, respectively (the onset of the peaks). T_1, T_H—the binary eutectic "THF hydrate–ice Ih" and the THF hydrate melting temperatures in the "THF–water–β-glycine" ternary system, respectively. T_L—liquidus melting temperatures in a concentration range with high THF content (the maximum of the peaks)

Fig. 8 Solvent crystal morphologies on horizontal cross section of frozen samples of aqueous glycine solution (**a**) and glycine solution in the THF/water co-solvent system (15 mass% (**b**); 20 mass% (**c**) of THF). *Scale bar* 500 μm
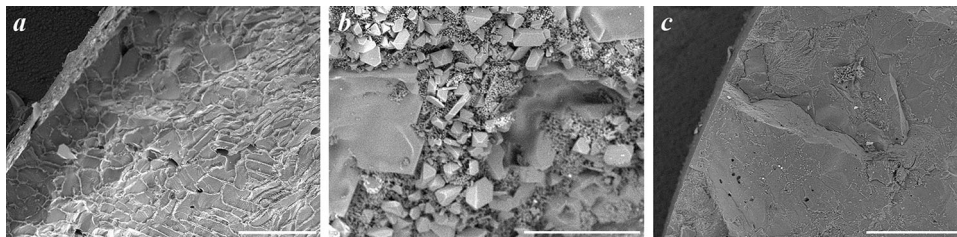
aqueous solutions of mannitol at low supercooling [45]. In the case of the sample with THF content corresponding to the THF hydrate composition (20 mass%) (Fig. 8c), individual crystals (<10 μm) are so small in size that they cannot be distinguished at the resolution used (×100–500). We consider this as an explanation of the fact that, according to [46], the onset of the hydrate formation in a solution with the stoichiometric water/THF mole ratio (17:1) occurs mostly inside the bulk liquid phase. For the sample with 15 mass% THF (Fig. 8b), the observed frozen structure corresponds to the close mixture of large THF hydrate crystals (truncated cubes/octahedrons) and of the crystals belonging to the solidus of the peritectic quadrangle (Fig. 7b3) THF hydrate–ice Ih–β-glycine (small and spherical).

The experiments on the pressure drop in the drying chamber as a function of THF content in the samples are illustrated in Fig. 9. These experiments have shown a significant shortening of the primary drying stage of frozen solutions of glycine in the THF–water co-solvent system as compared with aqueous solution: 135 min for THF–water (20 mass%) and 285 min for aqueous solution.

It was demonstrated in [7] that the addition of small amounts of TBA (up to 10 mass%) to sucrose solutions not only significantly shortens the primary drying stage, but also increases the specific surface of the prepared sucrose samples, when compared with aqueous solutions. The shortening of the primary drying stage in the TBA–water co-solvent system is attributed to the formation of the TBA hydrate, the change (decreasing) in the freezing temperature affecting the morphology of the frozen solution and resulting in higher dispersiveness of the product, lowered sublimation enthalpy of the solvent and increased saturated vapor pressure [5–8]. Keeping in mind the estimated value of the sublimation enthalpy of the THF hydrate, derived from literature data [47–49], we attribute the shortening of the primary drying stage to a smaller required heat transfer to the samples for a given shelf temperature ($\Delta_{sub}H$ for THF hydrate and ice Ih: 2370 and 2830 kJ kg^{-1}, respectively). It is well known for frozen aqueous solutions that the size of ice crystals must be large enough to obtain the shortest primary drying times (drying rates for slowly frozen samples typically greater than for fast frozen ones). Again, ice crystals must be smaller in size to produce a large specific surface area of the dried matrix in order to enable an easy desorption of unfrozen water from the pore surface to reduce secondary drying time [42, 44, 50]. In this case, however, it should be pointed out that the reduction of the sublimation enthalpy has a greater impact on reducing the drying time than the impact that a reduction in the size of crystallites has on increasing its duration. So, we suppose that in the case when freeze-drying process is rate
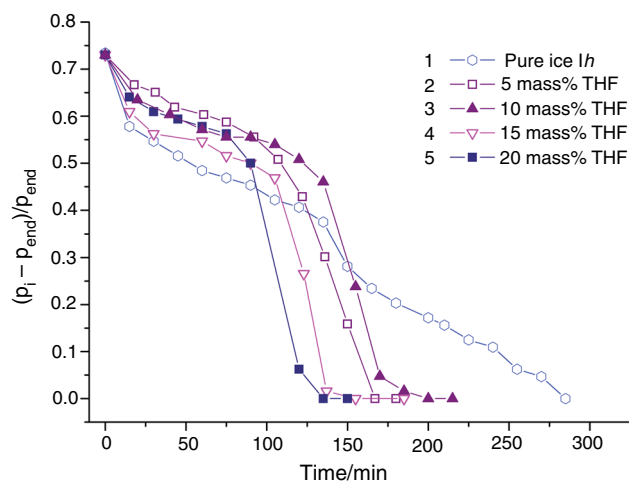
Fig. 9 Pressure decrease in the drying chamber as a function of solvent composition of the glycine solution [line "1"—pure water (ice I*h* is a single phase, removed by sublimation); line "2"— 5 mass% of THF; line "3"—10 mass% of THF; line "4"—15 mass% of THF; line "5"—20 mass% of THF (THF hydrate is a single phase, removed by sublimation)]. The *error bars* are smaller than the symbols themselves

limiting by the heat transfer (at very low product temperature), it would be of major importance for practical applications.

According to XRD data, in all samples obtained by freeze-drying, glycine was present as the metastable *β*-modification [51]. Visual inspection of the obtained sample revealed a stable freeze-dried cake lacking any signs of skin on the cake surface and collapsed inclusions near the bottom of the vial. At the same time, it should be noted that in some cases the upper part of the cake erupted from the vial (mass lost 7.1%) on freeze-drying glycine solutions in the THF–water co-solvent system (20 mass% of THF). In order to reduce sublimation rates, we carried out similar experiments at shelf temperature of 253 K. These

experiments also have shown a significant shortening of the primary drying stage with a slight decrease in mass loss (4.9%). Furthermore, a significant change in the internal structure of freeze-dried cakes occurred on replacement of pure ice I*h* with pure THF hydrate (20 mass% of THF) at the sublimation (removal) stage. According to SEM data (Fig. 10), it leads to a significant reduction of the particle size of glycine samples. We suppose that using the mannitol, trehalose or sucrose, which are able to form a mechanically strong cake [2, 30], can prevent the mass loss during primary drying. This will be the focus of future work.

It should also be pointed out that THF is categorized as a Class 2 solvent in the ICH Harmonized Tripartite Guideline on Impurities: Guidelines for Residual Solvents Q3C (R5) [5, 52], whose use is limited in pharmaceutical products because of their inherent toxicity (TBA is categorized as a Class 3, includes no solvent known as a human health hazard at levels normally accepted in pharmaceuticals). It should also be pointed out that the pharmaceutical product NAB-paxlitaxel (nanoparticles albumin-bound paxlitaxel, one of the most important drugs in the modern treatment of metastatic breast cancer, Abraxane® [53–55]), is currently on the market that has been manufactured with the use of methylene chloride or chloroform, other Class 2 solvents [53–57].

The "injectable nanoparticle generator", which spontaneously forms nanometer-sized doxorubicin-containing particles in aqueous solution, has been manufactured using dimethylformamide and methanol (Class 2 solvents) [58]. A cryogenic SFL process was developed to produce microparticulate powders consisting of an API molecularly embedded within a pharmaceutical excipient matrix; the samples have been manufactured using THF (Class 2 solvent) [59].

Fig. 10 SEM images of resulting cake structures of glycine samples, obtained by freeze-drying of glycine solution in the THF/water co-solvent system (20 mass% of THF) (**a–c**) and aqueous glycine solution (**d–f**). *Scale bar* **a**, **d** 50 μm; **b**, **e** 30 μm, and **c**, **f** 15 μm
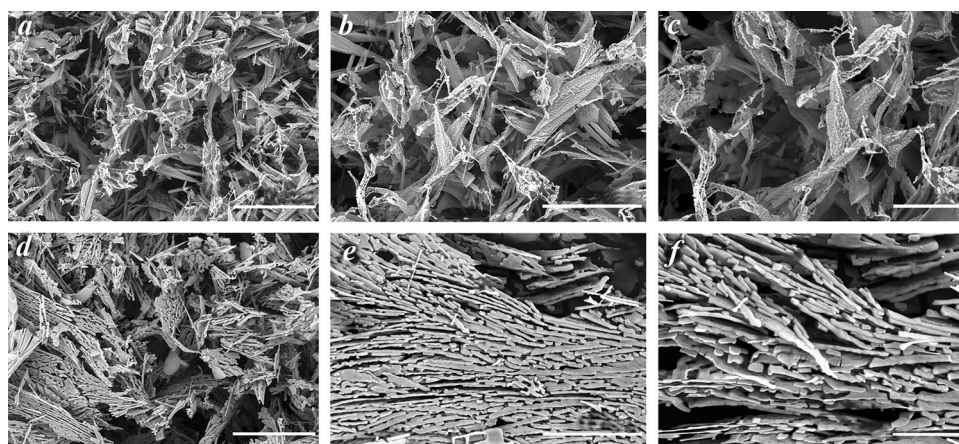
Conclusions

The THF hydrate crystallizes almost quantitatively on freezing from glycine solutions in the THF–water co-solvent system under conditions common for laboratory freeze-dryer. The substitution of a single-component solvent (water) with a two-component one (THF–water) does not affect the polymorphism of glycine. However, the substitution of sublimed ice Ih (pure water) for THF hydrate (co-solvent system of the composition corresponding to that of the clathrate hydrate) leads to a significant reduction of the particle size of glycine samples. Using a mixed solvent giving a clathrate on freezing is beneficial in terms of the significant shortening of the primary drying stage as compared with pure aqueous solutions and is of major importance for practical applications.

References

1. Oetjen GW, Haseley P. Freeze-drying. 2nd ed. Weinheim: Wiley; 2004.
2. Wang W. Lyophilization and development of solid protein pharmaceuticals. Int J Pharm. 2000;203:1–60.
3. Tang XC, Pikal MJ. Design of freeze-drying processes for pharmaceuticals: practical advice. Pharm Res. 2004;21:191–200.
4. Liu JS. Physical characterization of pharmaceutical formulations in frozen and freeze-dried solid states: techniques and applications in freeze-drying development. Pharm Dev Technol. 2006;11:3–28.
5. Teagarden DL, Baker DS. Practical aspects of lyophilization using non-aqueous co-solvent systems. Eur J Pharm Sci. 2002;15:115–33.
6. Vessot S, Andrieu J. A review on freeze drying of drugs with tert-butanol (TBA) + water systems: characteristics, advantages, drawbacks. Dry Technol. 2012;30:377–85.
7. Kasraian K, DeLuca PP. The effect of tertiary butyl alcohol on the resistance of the dry product layer during primary drying. Pharm Res. 1995;12:491–5.
8. Daoussi R, Vessot S, Andrieu J, Monnier O. Sublimation kinetics and sublimation end-point times during freeze-drying of pharmaceutical active principle with organic co-solvent formulations. Chem Eng Res Des. 2009;87:899–907.
9. Wanning S, Süverkrüp R, Lamprecht A. Pharmaceutical spray freeze drying. Int J Pharm. 2015;488:136–53.
10. Hu JH, Johnston KP, Williams RO. Spray freezing into liquid (SFL) particle engineering technology to enhance dissolution of poorly water soluble drugs: organic solvent versus organic/aqueous co-solvent systems. Eur J Pharm Sci. 2003;20:295–303.
11. Overhoff KA, Johnston KP, Tam J, Engstrom J, Williams RO. Use of thin film freezing to enable drug delivery: a review. J Drug Deliv Sci Technol. 2009;19:89–98.
12. Rasmussen DH, MacKenzie AP. Phase diagram for the system water–dimethylsulphoxide. Nature. 1968;220:1315–7.
13. Takaizumi K, Wakabayashi T. The freezing process in methanol-, ethanol-, and propanol-water systems as revealed by differential scanning calorimetry. J Solut Chem. 1997;26:927–39.
14. Dyadin YA, Bondaryuk IV, Zhurko FV. Clathrate hydrates at high pressures. In: Atwood JL, Davies JED, MacNicol DD, editors. Inclusion compounds, vol. 5. Oxford: Oxford University Press; 1991. p. 214–75.
15. Yu L, Milton N, Groleau EG, Mishra DS, Vansickle RE. Existence of a mannitol hydrate during freeze-drying and practical implications. J Pharm Sci. 1999;88:196–8.
16. Sundaramurthi P, Suryanarayanan R. Influence of crystallizing and non-crystallizing cosolutes on trehalose crystallization during freeze-drying. Pharm Res. 2010;27:2384–93.
17. Kasraian K, DeLuca PP. Thermal analysis of the tertiary butyl alcohol-water system and its implications on freeze-drying. Pharm Res. 1995;12:484–90.
18. Sloan ED, Koh CA. Clathrate hydrates of natural gases. 3rd ed. Boca Raton: CRC Press; 2008.
19. Sum AK, Koh CA, Sloan ED. Clathrate hydrates: from laboratory science to engineering practice. Ind Eng Chem Res. 2009;48:7457–65.
20. Lund DB, Fennema O, Powrie WD. Effect of gas hydrates and hydrate formers on invertase activity. Arch Biochem Biophys. 1969;129:181–8.
21. Booker RD, Koh CA, Sloan ED, Sum AK, Shalaev E, Singh SK. Xenon hydrate dissociation measurements with model protein systems. J Phys Chem B. 2011;115:10270–6.
22. Ogienko AG, Boldyreva EV, Manakov AY, Myz SA, Ogienko AA, Yunoshev AS, Zevak EG, Kutaev NV, Krasnikov AA. Preparation of fine powders of pharmaceutical substances by freeze-drying of frozen solutions in systems with clathrate formation. Dokl Phys Chem. 2012;444:88–92.
23. Zevak EG, Ogienko AG, Boldyreva EV, Myz SA, Ogienko AA, Kovalenko YE, Kolesov BA, Drebushchak VA, Trofimov NA, Krasnikov AA, Manakov AY, Boldyrev VV. Salbutamol-glycine composite microballs for pulmonary drug delivery. RDD Eur. 2013;2:329–34.
24. Teagarden DL, Wang W, Baker DS. Practical aspects of freeze-drying of pharmaceutical and biological products using non-aqueous co-solvent systems. In: Rey L, May JC, editors. Freeze drying/lyophilization of pharmaceutical and biological products. 3rd ed. London: Informa Healthcare; 2010. p. 254–87.
25. Cui JX, Li CL, Deng YJ, Wang YL, Wang W. Freeze-drying of liposomes using tertiary butyl alcohol/water co-solvent systems. Int J Pharm. 2006;312:131–6.
26. Oesterle J, Franks F, Auffret T. The influence of tertiary butyl alcohol and volatile salts on the sublimation of ice from frozen sucrose solutions: implications for freeze-drying. Pharm Dev Technol. 1998;3:175–83.
27. Park Y, Cha M, Shin W, Cha JH, Lee H, Ripmeester JA. Thermodynamic and spectroscopic analysis of tertbutyl alcohol hydrate: application for the methane gas storage and transportation. In: Proceedings of the 6th international conference on gas hydrates (ICGH 2008), Vancouver, British Columbia, Canada, 6–10 July 2008.
28. Wittaya-Areekul S, Nail SL. Freeze-drying of tert-butanol/water systems: effects of formulation and process variables on residual solvents. J Pharm Sci. 1998;87:491–5.
29. Wittaya-Areekul S, Needham G, Milton N, Roy ML, Nail SL. Freeze-drying of tert-butanol/water cosolvent systems: a case study in formation of friable freeze-dried powder of tobramycin sulfate. J Pharm Sci. 2002;91:1147–55.

30. Carpenter JF, Chang BS, Garzon-Rodriguez W, Randolph TW. Rational design of stable lyophilized protein formulations: theory and practice. In: Carpenter JF, Manning MC, editors. Rational design of stable protein formulations: theory and practice. Boston: Springer; 2002. p. 109–33.

31. Pyne A, Suryanarayanan R. Phase transitions of glycine in frozen aqueous solutions and during freeze-drying. Pharm Res. 2001;18:1448–54.

32. Chongprasert S, Knopp SA, Nail SL. Characterization of frozen solutions of glycine. J Pharm Sci. 2001;90:1720–8.

33. Surovtsev NV, Adichtchev SV, Malinovsky VK, Ogienko AG, Drebushchak VA, Manakov AY, Ancharov AI, Yunoshev AS, Boldyreva EV. Glycine phases formed from frozen aqueous solutions, revisited. J Chem Phys. 2012;137:065103.

34. Shalaev E, Franks F. Solid–liquid state diagrams in pharmaceutical lyophilisation: crystallisation of solutes. In: Levine H, editor. Progress in amorphous food and pharmaceutical systems. Cambridge: The Royal Society of Chemistry; 2002. p. 200–15.

35. Boldyreva EV, Drebushchak VA, Drebushchak TN, Paukov IE, Kovalevskaya YA, Shutova ES. Polymorphism of glycine: thermodynamic aspects. 1. Relative stability of the polymorphs. J Therm Anal Calorim. 2003;73:409–18.

36. Drebushchak VA, Ogienko AG, Boldyreva EV. Polymorphic effects and the eutectic melting in the H_2O-glycine system. J Therm Anal Calorim. 2013;111:2187–94.

37. Röttger K, Endriss A, Ihringer J, Doyle S, Kuhs WF. Lattice constants and thermal expansion of H_2O and D_2O ice Ih between 10 and 265 K. Acta Cryst B. 1994;50:644–8.

38. Ogienko AG, Kurnosov AV, Manakov AY, Larionov EG, Ancharov AI, Sheromov MA, Nesterov AN. Gas hydrates of argon and methane synthesized at high pressures: composition, thermal expansion, and self-preservation. J Phys Chem B. 2006;110:2840–6.

39. Hester KC, Huo Z, Ballard AL, Koh CA, Miller KT, Sloan ED. Thermal expansivity for sI and sII clathrate hydrates. J Phys Chem B. 2007;111:8830–5.

40. Lebedev BV, Rabinovich IB, Milov VI, Lityagov VY. Thermodynamic properties of tetrahydrofuran from 8 to 322 K. J ChemThermodyn. 1978;10:321–9.

41. Bhatnagar BS, Martin SM, Teagarden DL, Shalaev EY, Suryanarayanan R. Investigation of PEG crystallization in frozen PEG-sucrose-water solutions. I. Characterization of the nonequilibrium behavior during freeze-thawing. J Pharm Sci. 2010;99:2609–19.

42. Searles JA, Carpenter JF, Randolph TW. The ice nucleation temperature determines the primary drying rate of lyophilization for samples frozen on a temperature-controlled shelf. J Pharm Sci. 2001;90:860–71.

43. Liu J, Viverette T, Virgin M, Anderson M, Dalal P. A study of the impact of freezing on the lyophilization of a concentrated formulation with a high fill depth. Pharm Dev Technol. 2005;10:261–72.

44. Hottot A, Vessot S, Andrieu J. Freeze drying of pharmaceuticals in vials: influence of freezing protocol and sample configuration on ice morphology and freeze-dried cake texture. Chem Eng Process. 2007;46:666–74.

45. Nakagawa K, Hottot A, Vessot S, Andrieu J. Influence of controlled nucleation by ultrasounds on ice morphology of frozen formulations for pharmaceutical proteins freeze-drying. Chem Eng Process. 2006;45:783–91.

46. Zhang W, Creek JL, Koh CA. A novel multiple cell photo-sensor instrument: principles and application to the study of THF hydrate formation. Meas Sci Technol. 2001;12:1620–30.

47. Handa YP. Enthalpies of fusion and heat capacities for $H_2^{18}O$ ice and $H_2^{18}O$ tetrahydrofuran clathrate hydrate in the range 100–270 K. Can J Chem. 1984;62:1659–61.

48. Tombari E, Presto S, Salvetti G, Johari GP. Heat capacity of tetrahydrofuran clathrate hydrate and of its components, and the clathrate formation from supercooled melt. J Chem Phys. 2006;124:154507.

49. Hossenlopp IA, Scott DW. Heat capacities and enthalpies of vaporization of six organic compounds. J Chem Thermodyn. 1981;13:405–14.

50. Liapis AI, Bruttini R. Freeze Drying. In: Mujumdar AS, editor. Handbook of industrial drying. 2nd ed. New York: Marcel Dekker Inc; 1995. p. 309–44.

51. Drebushchak TN, Boldyreva EV, Shutova ES. β-glycine. Acta Cryst E. 2002;58:o634–6.

52. http://www.fda.gov/downloads/drugs/guidancecomplianceregulatoryinformation/guidances/ucm073394.pdf.

53. Gupta RB. Polymer or protein stabilized nanoparticles from emulsions. In: Gupta RB, Kompella UB, editors. Nanoparticle technology for drug delivery. New York: CRC Press; 2006. p. 85–102.

54. Harries M, Ellis P, Harper P. Nanoparticle albumin-bound paclitaxel for metastatic breast cancer. J Clin Oncol. 2005;23:7768–71.

55. Fu Q, Sun J, Zhang WP, Sui XF, Yan ZT, He ZG. Nanoparticle albumin-bound (NAB) technology is a promising method for anti-cancer drug delivery. Recent Pat Anticancer Drug Discov. 2009;4:262–72.

56. Kratz F. Albumin as a drug carrier: design of prodrugs, drug conjugates and nanoparticles. J Control Release. 2008;132:171–83.

57. Yi XL, Lian XH, Dong JX, Wan ZY, Xia CY, Song X, Fu Y, Gong T, Zhang Z. Co-delivery of pirarubicin and paclitaxel by human serum albumin nanoparticles to enhance antitumor effect and reduce systemic toxicity in breast cancers. Mol Pharm. 2015;12:4085–98.

58. Xu R, Zhang G, Mai J, Deng X, Segura-Ibarra V, Wu S, Shen J, Liu H, Hu Z, Chen L, Huang Y, Koay E, Huang Y, Liu J, Ensor JE, Blanco E, Liu X, Ferrari M, Shen H. An injectable nanoparticle generator enhances delivery of cancer therapeutics. Nat Biotechnol. 2016;34:414–8.

59. Rogers TL, Nelsen AC, Hu JH, Brown JN, Sarkari M, Young TJ, Johnston KP, Williams RO. A novel particle engineering technology to enhance dissolution of poorly water soluble drugs: spray-freezing into liquid. Eur J Pharm Biopharm. 2002;54:271–80.